34. MAGNETIC PROPERTIES OF BASALT SAMPLES FROM DEEP SEA DRILLING PROJECT HOLES 597B AND 597C[1]

Tadashi Nishitani, Institute of Mining Geology, Mining College, Akita University[2]

ABSTRACT

Measurements of magnetic properties were made on basalt samples recovered from Holes 597B and 597C. This paper describes the intensity and inclination of natural remanent magnetization (NRM), the intensity of anhysteretic remanent magnetization (ARM), the median demagnetizing field (MDF) for NRM and ARM, the initial susceptibility, the Koenigsberger ratio (Q). The mean inclinations (I) after alternating field demagnetization for Holes 597B and 597C are 45.4 ± 7.1° and 45.0 ± 7.6°, respectively. These numeric quantities are greater than the calculated value of I = 34° expected at this site. A change of magnetic properties occurs at the depths of 100 and 120 m, respectively, which coincide with the boundaries between major petrological units.

INTRODUCTION

Site 597 (18°48′S, 129°45′W) is located west of the East Pacific Rise in crust of late Oligocene age (Fig. 1). Seafloor depth is about 4160 m. During Leg 92, basement was cored in Holes 597B and 597C, which were located less than 50 m apart. At Hole 597B, 5.43 m of basalt were recovered, and at Hole 597C, 55.2 m. One or two oriented samples (2.54 cm in diameter) were taken from every section of each core, for a total of 69 samples, to use for measurement of magnetic properties.

The magnetic properties reported here are the intensity and inclination of natural remanent magnetization (NRM), the intensity of anhysteretic remanent magnetization (ARM), the median demagnetizing field (MDF) for NRM and ARM, the initial susceptibility, and the Koenigsberger ratio (Q).

EXPERIMENTAL PROCEDURE

In total, 11 samples from Hole 597B and 58 samples from Hole 597C were investigated. NRM intensity and inclination were measured with a spinner magnetometer. The noise level of the magnetometer was less than 10^{-7} emu/cm^3. The initial susceptibility was measured by using a Bison Model 3101 susceptibility meter. NRM intensity, inclination, and the initial susceptibility were measured by using standard specimens (2.54 cm in diameter and 1.9 to 2.5 cm in length). After these measurements were taken, each minicore was sliced into two disks with nearly equal volumes. One disk from each minicore was demagnetized with a peak alternating field (AF) of up to 900 Oe. A single-axis AF demagnetizer was used. ARM was measured on specimens using a peak AF of 900 Oe (90 mT) and a direct field of 0.4 Oe. Stepwise AF demagnetization was carried out again to 900 Oe. The median demagnetizing field was determined for both NRM and ARM.

RESULTS

The results of the measurements are listed in Table 1. The following magnetic properties are listed: NRM intensity, MDF of NRM, susceptibility (χ), Koenigsberger ratio (Q), ARM intensity, MDF of ARM, NRM inclination, stable inclination, NRM declination, optimum demagnetizing field (ODF) of NRM, and sub-bottom depth. The Koenigsberger ratio is defined as the ratio of the intensity of NRM (J_n) to that induced by the Earth's magnetic field at the sampling site and is given by

$$Q = J_n/\chi H$$

where χ is the initial susceptibility and H is a constant calculated to be 0.36 Oe at Holes 597B and 597C.

NRM Intensity and Inclination

The intensities of NRM, inclinations, susceptibilities, and Q values are plotted as a function of depth in Figures 2 and 3. The average NRM intensity and susceptibilities in Hole 597B are $1.60 \pm 1.02 \times 10^{-3}$ emu/cm^3 and $1.46 \pm 1.17 \times 10^{-3}$ emu/cm$^3 \cdot$ Oe. The average NRM intensity in Hole 597C is $3.61 \pm 2.51 \times 10^{-3}$ emu/cm^3, about twice the level of intensity found in Hole 597B. Intensity in Hole 597C decreases slowly downhole from a peak value at 65 m, with the exception of the sharp peaks found in Samples 597C-7-2, 94 cm, and 597C-7-4, 97 m.

The numeric values of intensity of each parameter are compared to investigate the relationship between Holes 597B and 597C. The depth of Hole 597B is about 65 m, so the values from Hole 597C are averaged to about 65 m (from Sample 597C-3-1, 21–24 cm, to 597C-4-1, 60–63 cm. The mean magnetic properties for the upper 7 samples from Hole 597C are listed in Table 2. These nearly agree with those obtained in Hole 597B. Therefore, it is possible that the magnetic properties of Hole 597B correspond to those of the upper part (55.7 to 65 m) of Hole 597C. Magnetic properties are almost the same laterally, at a distance of about 50 m between Holes 597B and 597C.

All samples were demagnetized up to 900 Oe. In general, inclinations decrease at depths from 55 to 73 m where the AF peak field increases (Fig. 4). From 73 to 100 m, magnetizations are more stable than those of the upper part (Fig. 5). Below 100 m, inclinations only slightly deviate from the alternating field (Figs. 6, 7, and 8).

[1] Leinen, M., Rea, D. K., et al., *Init. Repts. DSDP*, 92: Washington (U.S. Govt. Printing Office).
[2] Address: Institute of Mining Geology, Mining College, Akita University, Akita 010, Japan.

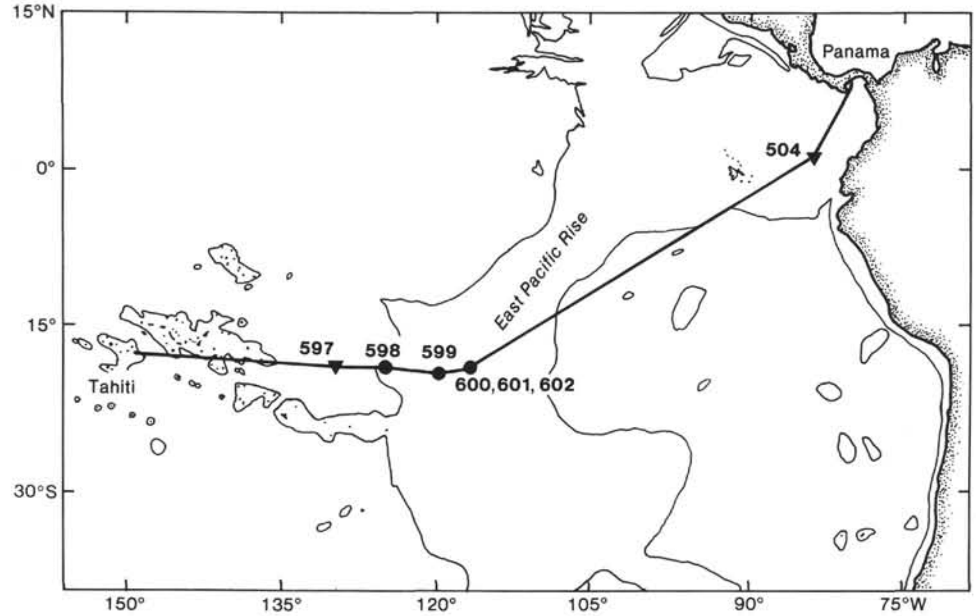

Figure 1. Location of Site 597, DSDP Leg 92. Inverted triangle denotes re-entry.

The amount of inclination is stable at a certain level of demagnetization, which is thus distinguished as the best method of magnetic cleaning and is termed the *optimum demagnetizing field* (ODF) for the alternating field demagnetization method.

ARM Measurement

Mean ARM intensities are $2.71 \pm 0.66 \times 10^{-3}$ emu/cm^3 for Hole 597B and $2.71 \pm 0.69 \times 10^{-3}$ emu/cm^3 for Hole 597C; their deviation is not very large. The variation of ARM intensity corresponds to the variation of NRM intensity. Figure 9 shows the relationship between NRM and ARM intensity. Alternating field demagnetization of ARM was performed. The stability (MDF) of ARM shows considerable variation: from 36 to 353 Oe. The mean MDF of Holes 597B and 597C are 129 ± 43 and 113 ± 72 Oe, respectively. The MDF of NRM and the MDF of ARM show good correlation and their peaks coincide (Figs. 10 and 11).

DISCUSSION

A positive inclination indicates reversed polarity at this latitude (18°48′S). All samples showed reversed polarity except at two depths (597C-7-4, 137–140 cm and 597C-7-5, 70–73 cm). These most likely indicate the normal interval between Anomalies 8 and 9. This would imply an age of 28.5 Ma for Site 597 (Harland et al., 1982); this age is consistent with that determined from the study of nannofossils from the site (Knüttel, this volume). The mean inclinations, after AF demagnetization, for Holes 597B and 597C are $45.4 \pm 7.1°$ and $45.0 \pm 7.6°$, respectively. These values are greater than the calculated value of $I = 34°$ expected at this site, assuming a dipolar field. Unusually high inclination values are also reported at Sites 319 and 320 on the Galapagos Rise (Ade-Hall and Johnson, 1976), perhaps for these same basic reasons. High inclination values suggest that basalts in Holes 597B and 597C were generated at 26.6°S and moved northward to the present position. Marshall (1978) reported that remanence inclinations at the North Pacific sites differ considerably from the present geomagnetic field inclination and suggested a northward motion of the Pacific crust. Hammond et al. (1974) showed northward movement of the Central Pacific Basin, and Francheteau et al. (1970) indicated that the Pacific crust migrated northward about 30°. However, shallow inclination values were observed in Holes 332A, 332B, 396, and 396A in the Atlantic (Ryall et al., 1977). Therefore, high inclination values at Holes 597B and 597C are not a global feature, but may be a local characteristic of the Pacific area. Other mechanisms proposed to explain this discrepancy include tectonic rotation, secular variation, geomagnetic excursions, or a change in NRM.

Figures 3 and 10 indicate that the magnetic properties show a large change at about 100 m depth, particularly the MDF of NRM and ARM and the Q value. Above 100 m the Q value shows extreme variation, but it is constant below 100 m. The stability of NRM and ARM decreases gradually as the depth increases from 55 to 100 m, and it increases abruptly at approximately 100 m. It decreases again as depth increases to 120 m and increases at depths below 120 m. A change of magnetic properties occurs at 100 m and 120 m, which coincides with the boundaries between major geochemical and petrological units (Pearce et al., this volume).

The NRM intensity increased in particular after the inclination change occurred. Other magnetic properties, susceptibilities and Q values do not show such unusual variations. We can therefore assume that the intensity of the magnetic field increased significantly just after the magnetic reversals occurred.

REFERENCES

Ade-Hall, J. M., and Johnson, H. P., 1976. Paleomagnetism of basalts, Leg 34. *In* Yeats, R. S., Hart, S. R., et al., *Init. Repts. DSDP*, 34: Washington (U.S. Govt. Printing Office), 513–532.

Francheteau, J., Harrison, C. G. A., Sclater, J. G., and Richards, M. L., 1970. Magnetization of Pacific seamounts: a preliminary polar curve for the northeastern Pacific. *J. Geophys. Res.*, 75:2035–2061.

Hammond, S. R., Theyer, F., and Sutton, G. H., 1974. Paleomagnetic evidence of northward movement of the Pacific Plate in deep-sea cores from the central Pacific Basin. *Earth Planet. Sci. Lett.*, 22: 22–28.

Harland, W. B., Cox, A. V., Llewellyn, P. G., Pickton, C. A. G., Smith, A. G., and Walters, R., 1982. *A Geologic Time Scale*: Cambridge (Cambridge Univ. Press).

Marshall, M., 1978. The magnetic properties of some DSDP basalts from the North Pacific and inferences for Pacific plate tectonics. *J. Geophys. Res.*, 83:289–308.

Ryall, P. J. C., Hall, J. M., Clark, J., and Milligan, T., 1977. Magnetization of oceanic crustal layer 2: results and thoughts after DSDP Leg 37. *Can. J. Earth Sci.*, 14:684–706.

Date of Initial Receipt: 15 November 1984
Date of Acceptance: 26 December 1984

Table 1. Magnetic properties of basalt samples from Holes 597B and 597C.

Core-Section (interval in cm)	Piece	NRM intensity (emu/cm^3) × 10^{-3}	MDF of NRM (Oe)	Susceptibility (emu/cm^3 · Oe) × 10^{-3}	Q[a]	ARM intensity (emu/cm^3) × 10^{-3}	MDF of ARM (Oe)	NRM inclination (°)	Stable inclination (°)	NRM declination (°)[b]	ODF of NRM[c] (Oe)	Sub-bottom depth (m)
Hole 597B												
2-1, 17–20	1A	1.34	195	1.03	3.64	2.75	155	66.5	53.3	121.8	150	54.59
2-1, 83–85	5B	0.82	179	0.76	3.02	2.67	152	65.2	53.6	322.9	200	55.24
2-2, 45–48	2	0.26	146	1.25	0.57	2.04	134	56.7	41.0	276.0	100	56.37
2-2, 110–113	7B	1.99	128	0.51	10.93	3.34	151	65.4	44.1	321.9	150	57.02
2-2, 131–134	9	0.88	117	1.86	1.32	2.49	111	47.5	46.1	129.9	125	57.23
2-3, 29–32	3A	0.94	119	0.55	4.68	2.50	173	63.3	46.9	85.1	150	57.71
2-3, 114–117	12	2.20	91	0.55	11.16	4.42	111	73.4	57.4	9.7	150	58.56
3-1, 3-6	1	2.29	78	3.28	1.94	2.33	86	62.9	44.7	58.7	125	63.55
3-1, 132–135	8	1.33	151	0.39	9.56	2.66	196	41.5	40.5	61.1	125	64.84
3-2, 23–26	1B	1.50	108	2.05	2.03	2.16	107	53.0	35.3	305.8	150	65.25
3-2, 40–43	2	4.02	46	3.80	2.94	2.50	42	61.7	36.7	311.5	125	65.42
Hole 597C												
3-1, 21–24	2	1.55	265	0.62	6.90	2.75	175	53.8	45.7	172.4	300	55.73
3-1, 131–134	7	1.75	91	2.43	2.00	3.09	96	68.9	50.1	137.1	100	56.83
3-2, 40–43	2B	4.14	74	4.56	2.52	2.42	53	55.2	36.5	326.8	150	57.42
3-2, 143–146	5B	0.53	114	0.39	3.76	2.59	213	31.3	—	—	—	58.45
3-3, 5–8	1	0.89	140	0.43	5.72	2.72	172	72.2	60.1	126.5	150	58.57
3-3, 52–55	3	0.69	160	0.41	4.71	2.49	177	56.9	31.2	285.8	200	59.04
4-1, 60–63	1D	3.75	216	0.77	13.44	4.14	138	51.3	37.9	342.7	150	65.12
4-1, 120–123	1G	6.70	46	3.25	5.73	3.29	52	58.9	41.3	242.3	100	65.72
4-2, 21–24	2A	7.12	57	4.75	4.17	3.13	44	59.7	48.2	16.9	100	66.22
4-2, 111–114	5B	3.77	45	2.71	3.87	2.94	60	84.4	55.8	281.3	100	67.13
4-3, 27–30	1B	5.99	49	4.11	4.05	3.27	43	81.4	60.4	75.3	75	67.79
4-3, 91–94	3B	5.27	40	4.59	3.19	2.72	39	73.2	61.0	39.4	75	68.43
4-4, 23–26	1B	5.15	45	4.65	3.08	2.66	41	67.6	44.9	332.8	150	69.25
4-4, 76–79	2C	3.18	210	1.60	5.51	3.33	353	54.6	48.5	331.7	200	69.78
4-5, 26–29	3	4.72	37	3.80	3.45	2.29	36	58.1	45.3	16.1	75	70.78
4-5, 71–74	5A	3.10	64	5.70	1.51	2.26	37	56.7	45.6	6.8	75	71.22
4-6, 21–24	2	4.05	42	5.19	2.16	2.32	46	82.7	65.7	12.3	50	72.22
4-6, 73–76	5	1.14	160	0.39	8.02	2.00	175	46.2	43.0	0.0	200	72.75
5-1, 129–132	18	0.97	143	0.38	7.00	2.61	198	51.0	41.0	311.4	100	74.81
5-2, 63–66	7	3.93	133	0.52	20.87	3.95	163	49.9	46.1	24.7	150	75.64
6-1, 109–112	12A	4.25	186	0.89	13.21	3.60	190	50.5	50.6	343.2	125	83.61
6-2, 49–52	4	1.47	79	2.07	1.97	2.32	94	47.7	46.5	29.6	125	84.51
6-3, 62–65	3	3.51	54	3.32	2.93	2.28	55	71.2	49.3	45.9	100	86.14
6-4, 74–77	1L	3.38	59	2.43	3.87	3.04	75	71.3	37.8	273.5	125	87.76
6-5, 58–61	4E	2.66	146	0.74	10.01	3.29	119	37.8	37.9	3.6	200	89.10
7-1, 115–118	3D	5.86	74	3.40	4.79	3.10	52	75.9	50.2	130.2	150	92.67
7-2, 16–18	1B	7.22	128	3.55	5.66	3.25	72	51.8	45.6	355.5	150	93.17
7-2, 117–120	4B	11.57	74	2.86	11.23	3.69	77	60.3	50.6	206.6	150	94.18
7-4, 18–21	2A	6.04	51	1.54	10.91	2.98	49	67.6	54.0	56.6	100	96.20
7-4, 87–90	8B	14.51	91	3.80	10.62	4.43	82	56.8	50.2	280.7	125	96.89
7-4, 111–114	10A	6.42	67	3.31	5.38	2.80	72	70.4	56.0	210.6	125	97.13
7-4, 137–140	11	3.56	48	4.52	2.19	1.90	40	−56.9	−41.1	348.8	100	97.39
7-5, 70–73	7	2.70	41	4.61	1.63	2.23	36	−85.3	−76.7	71.4	75	98.22
8-1, 9–11	1A	1.56	35	4.01	1.08	3.15	86	60.1	41.9	328.9	300	100.60
8-1, 94–97	2A	3.61	296	3.32	3.02	3.15	170	56.9	41.0	80.7	250	101.46
8-2, 50–53	1B	4.31	196	3.18	3.77	2.82	171	51.2	39.1	57.6	400	102.51
8-3, 5–8	1	3.63	241	3.04	3.32	2.52	198	44.0	36.5	236.9	300	103.57
8-3, 130–133	9B	1.94	117	3.81	1.41	2.49	145	54.2	22.1	128.2	100	104.82
8-4, 102–105	6B	3.36	160	4.30	2.17	2.61	115	47.8	40.2	50.0	150	106.04
8-5, 60–63	1E	3.80	160	4.46	2.37	2.73	85	36.8	37.0	341.2	125	107.12
8-6, 56–59	1E	2.09	109	4.61	1.26	3.32	83	43.3	40.9	25.4	300	108.58
8-7, 9–12	1A	2.69	188	4.15	1.80	2.89	113	40.9	44.0	350.3	150	109.61
9-1, 9–12	1	4.04	109	5.92	1.90	3.76	164	51.5	36.5	7.0	150	109.61
9-1, 142–145	6C	3.06	167	4.12	2.06	3.19	152	51.6	38.9	336.8	200	110.93
9-2, 70–73	4B	3.87	136	5.01	2.15	3.37	164	65.2	41.6	228.6	250	111.72
9-3, 88–91	1F	2.23	113	4.81	1.29	2.93	146	82.9	47.3	160.9	125	113.39
9-4, 103–106	4E	6.19	123	5.18	3.32	3.07	141	45.5	41.9	4.5	150	115.05
10-1, 112–115	9B	3.23	241	4.36	2.06	2.86	129	50.1	40.1	294.5	200	119.64
10-2, 104–107	1H	3.14	51	5.24	1.67	1.85	40	54.0	43.6	8.8	300	121.06
10-3, 94–97	1G	2.26	95	4.05	1.55	1.97	45	54.4	43.9	353.7	125	122.46
10-4, 91–94	2A	1.36	49	2.93	1.29	1.48	50	53.5	52.6	26.0	350	123.93
10-5, 84–87	1E	1.68	129	2.84	1.64	1.57	53	49.7	46.4	355.6	125	125.36
10-6, 36–39	1C	1.94	240	3.80	1.42	1.69	52	61.0	40.5	327.2	200	126.38
10-7, 42–45	1C	1.74	254	3.16	1.53	1.56	84	65.4	42.2	344.6	200	127.93
11-1, 79–82	2D	1.05	197	3.12	0.94	1.55	92	54.9	47.1	36.0	125	128.31
11-2, 103–106	2	1.85	428	2.04	2.52	1.58	196	60.5	43.8	228.9	150	130.05
11-3, 13–15	1A	1.50	464	1.93	2.16	1.55	305	44.8	45.6	38.0	150	130.64
11-4, 62–64	4	1.47	466	1.84	2.21	1.68	267	53.7	42.9	105.2	200	132.63

[a] $Q = J_n/\chi H$, where J_n is an intensity of NRM, χ is susceptibility, and H = 0.36 Oe.
[b] Declination of NRM is listed only for reference.
[c] ODF means optimum demagnetizing field.

Table 2. Average magnetic properties from Holes 597B and 597C.

	Hole 597B[a] (54.59–65.42 m)	Hole 597C[b] (55.73–65.12 m)	Hole 597C[c] (55.73–132.63 m)
NRM intensity (emu/cm^3) × 10^{-3}	1.60 ± 1.02	1.90 ± 1.47	3.61 ± 2.51
MDF of NRM (Oe)	123 ± 43	151 ± 69	137 ± 101
Susceptibility (emu/cm^3) × 10^{-3}	1.46 ± 1.17	1.37 ± 1.58	3.16 ± 1.56
Q	4.71 ± 3.93	5.58 ± 3.87	4.24 ± 3.81
ARM intensity (emu/cm^3) × 10^{-3}	2.71 ± 0.66	2.89 ± 0.59	2.71 ± 0.69
MDF of ARM (Oe)	129 ± 43	146 ± 55	113 ± 72
NRM inclination (°)	59.7 ± 9.3	55.7 ± 13.3	57.3 ± 11.9
Stable inclination (°)	45.4 ± 7.1	43.6 ± 10.5	45.0 ± 7.6
ODF of NRM (Oe)	141 ± 26	175 ± 69	162 ± 75

[a] Mean value of all Hole 597B samples (n = 11).
[b] Mean value of upper part of Hole 597C samples (n = 7).
[c] Mean value of all Hole 597C samples (n = 58).

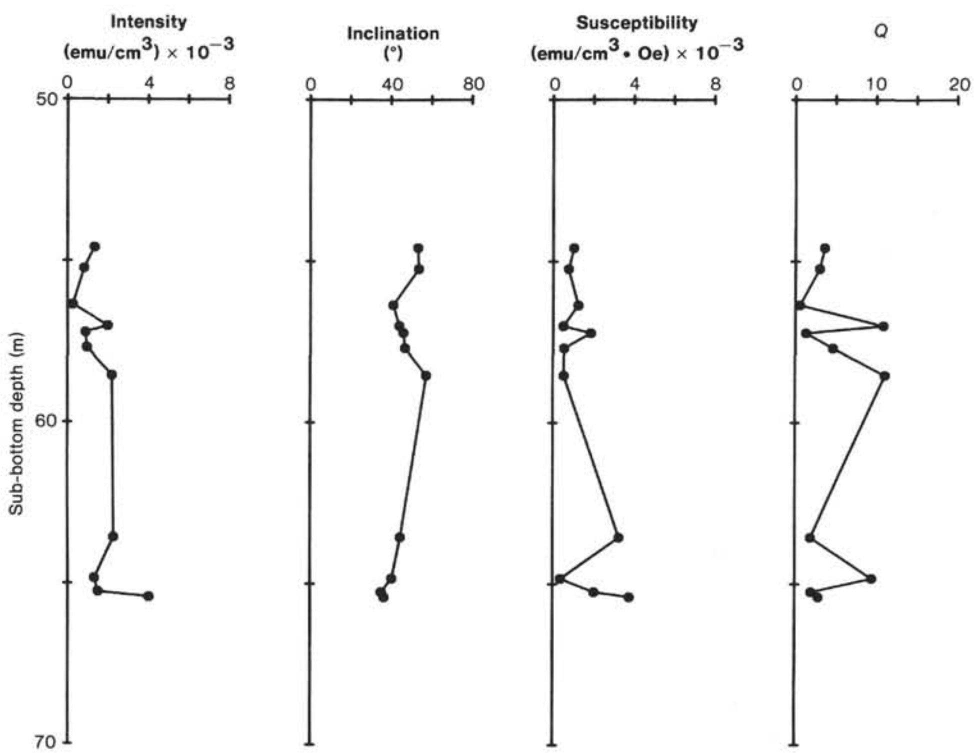

Figure 2. Intensity of NRM, inclinations after AF demagnetization, susceptibilities and Q values (H = 0.36 Oe) for Hole 597B plotted against sub-bottom depth.

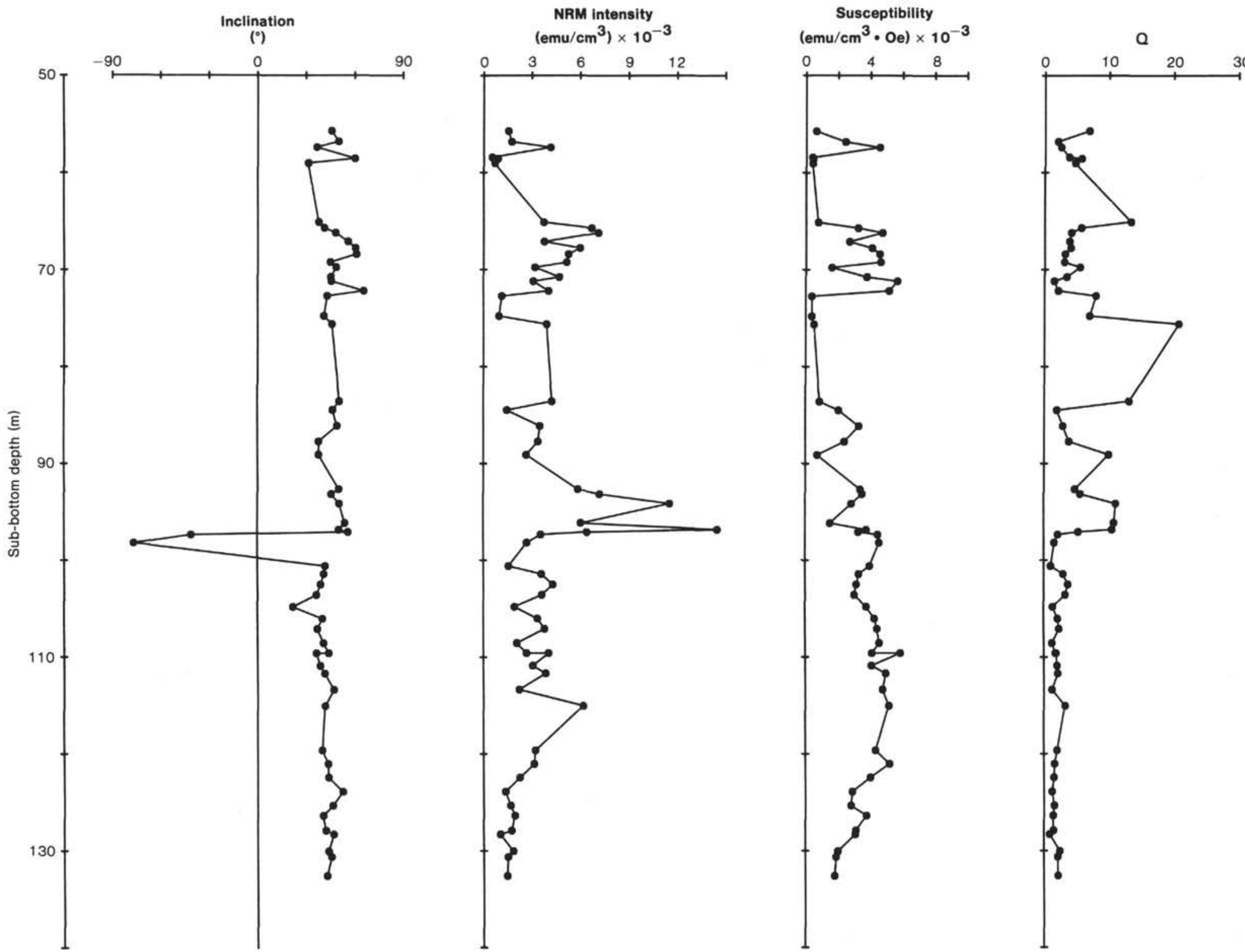

Figure 3. Inclinations after AF demagnetization, intensities, susceptibilities, and Q values (H = 0.36 Oe) for Hole 597C plotted against sub-bottom depth.

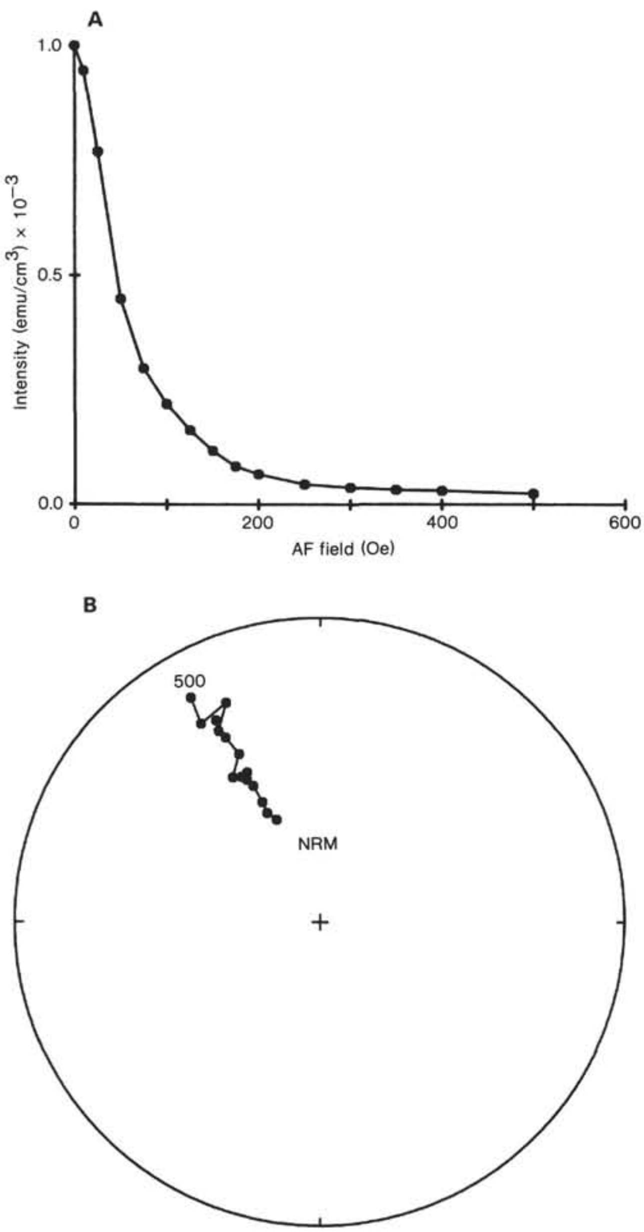

Figure 4. Results of AF demagnetization for Sample 597C-4-1, 120–123 cm. A. Change in intensities. B. Change in direction of NRM.

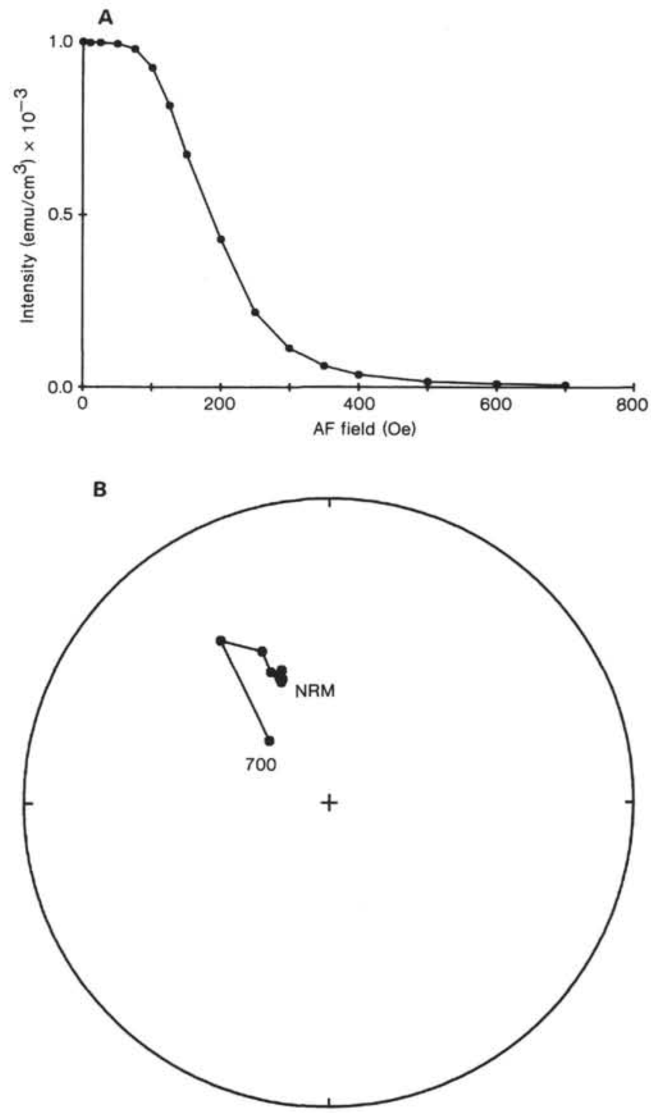

Figure 5. Results of AF demagnetization for Sample 597C-6-1, 109–112 cm. A. Change in intensity. B. Change in direction of NRM.

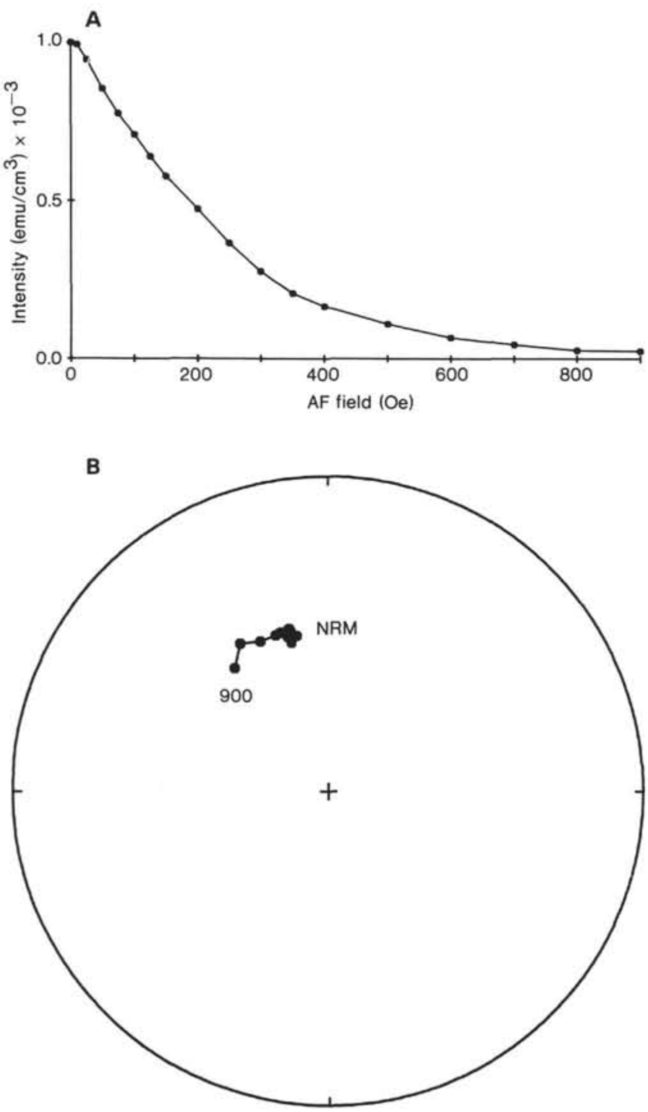

Figure 6. Results of AF demagnetization for Sample 597C-8-7, 9–12 cm. A. Change in intensity. B. Change in direction of NRM.

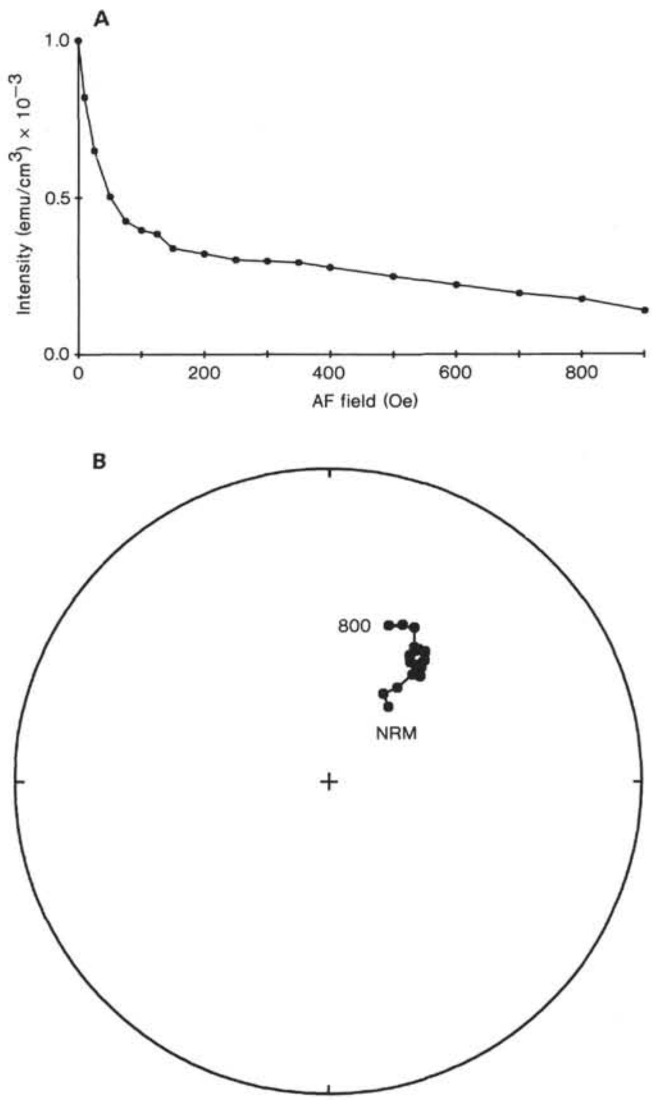

Figure 7. Results of AF demagnetization for Sample 597C-10-2, 104–107 cm. A. Change in intensity B. Change in direction of NRM.

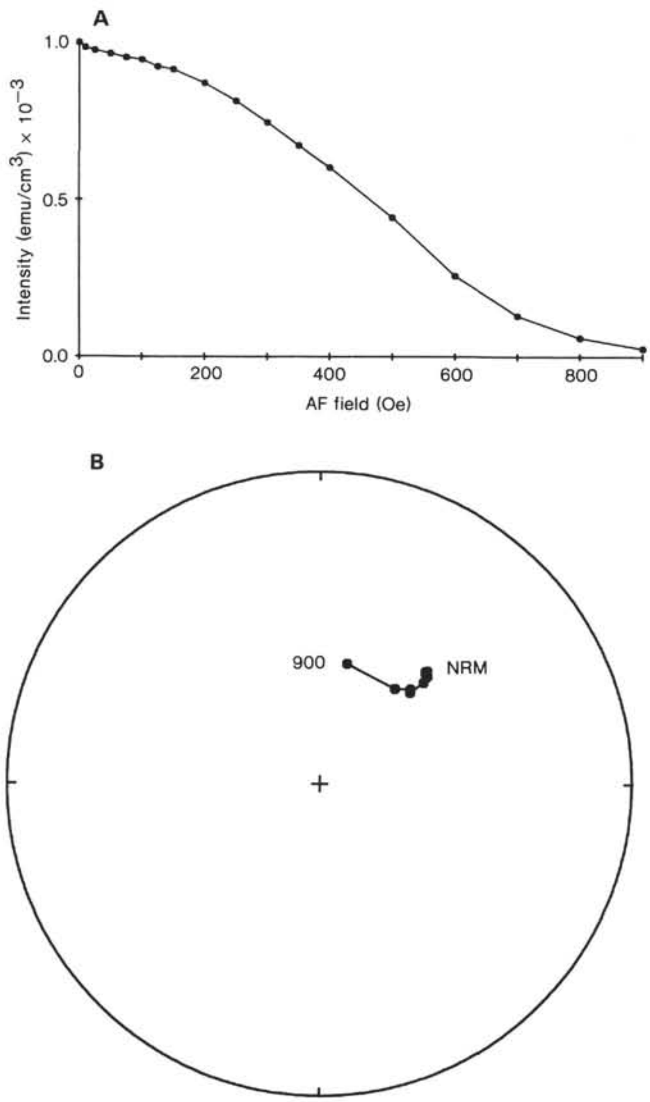

Figure 8. Results of AF demagnetization for Sample 597C-11-3, 13–15 cm. A. Change in intensity. B. Change in direction of NRM.

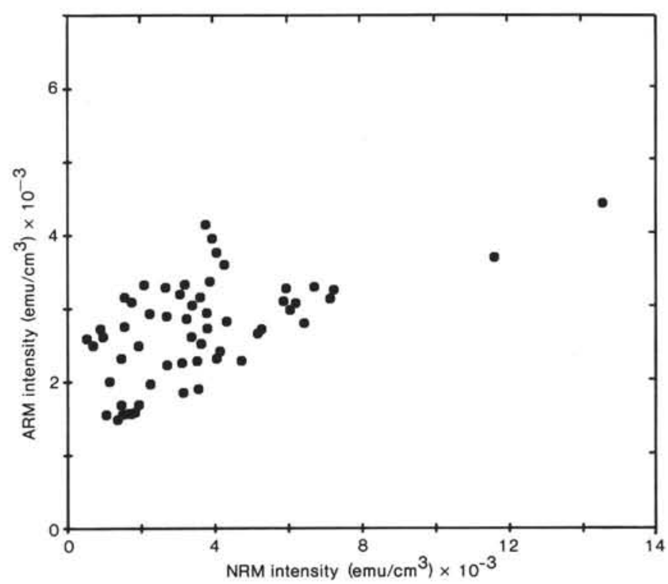

Figure 9. Relationship between NRM intensity and ARM intensity.

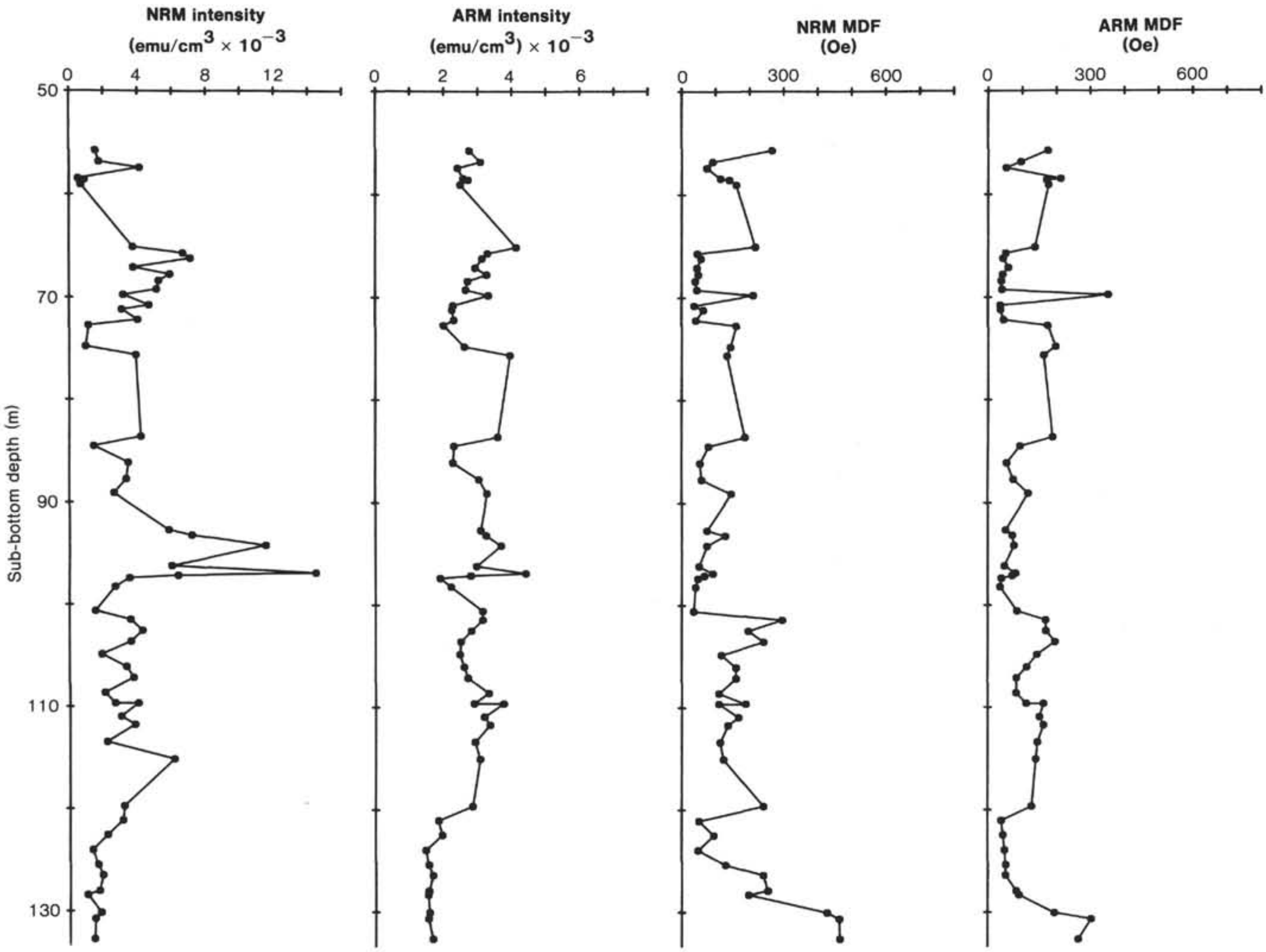

Figure 10. Intensity and MDF of NRM and of ARM as a function of sub-bottom depth at Site 597C.

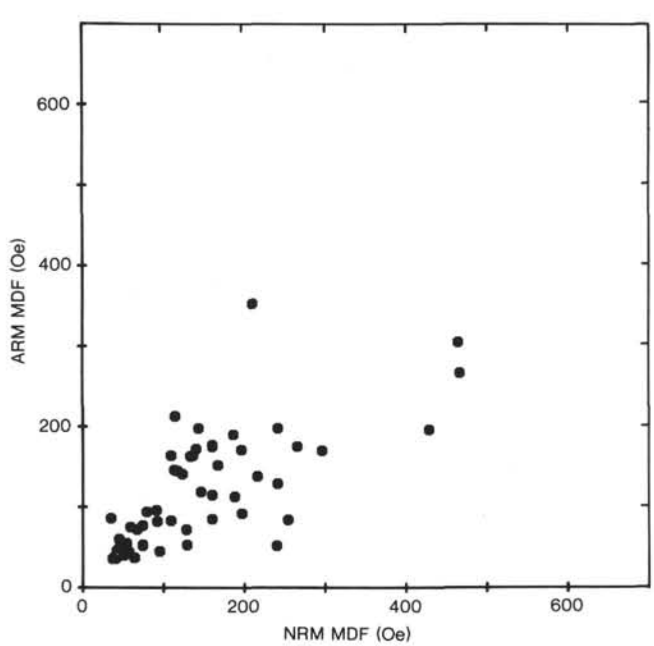

Figure 11. Relationship between MDF of NRM and of ARM.